Supporting Information

Increased Active Sites on Irregular Morphological α-Fe_2O_3 Nanorods for Enhanced Photoelectrochemical Performance

Jiawei Sun[a], Weiwei Xia[a*], Qian Zheng[a], Xianghua Zeng[a,b*],Wei Liu [c], Gang Liu[a], Pengdi Wang[a]

[a] *College of Physics Science and Technology & Institute of Optoelectronic Technology, Yangzhou University, Yangzhou 225002, P.R. China*

[b] *College of Electrical, Energy and Power Engineering, Yangzhou University, Yangzhou 225127, P. R. China*

[c] *State Key Laboratory of Bioelectronics, School of Biological Sciences & Medical Engineering, Southeast University, Nanjing 210096, P. R. China*

Supporting Information

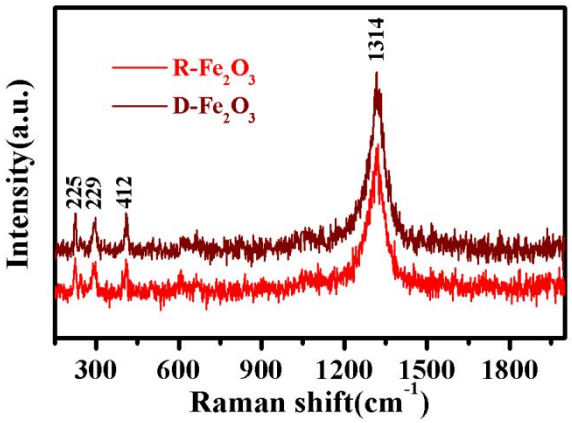

* *Corresponding authors. Email: xhzeng@yzu.edu.cn*

Figure S1. Raman spectra of as obtained R-Fe_2O_3 and D-Fe_2O_3 nanostructured arrays.

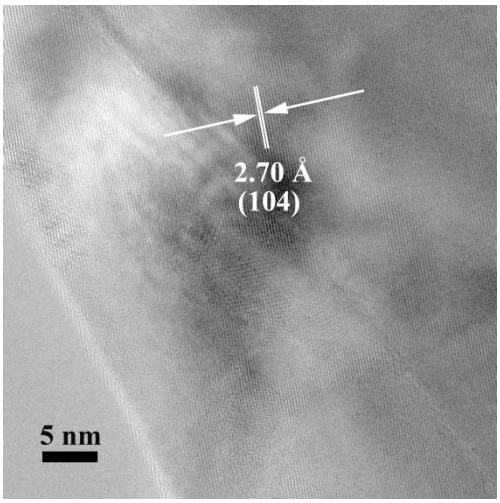

Figure S2. High-magnification image of a selected individual R-Fe_2O_3 nanorod.

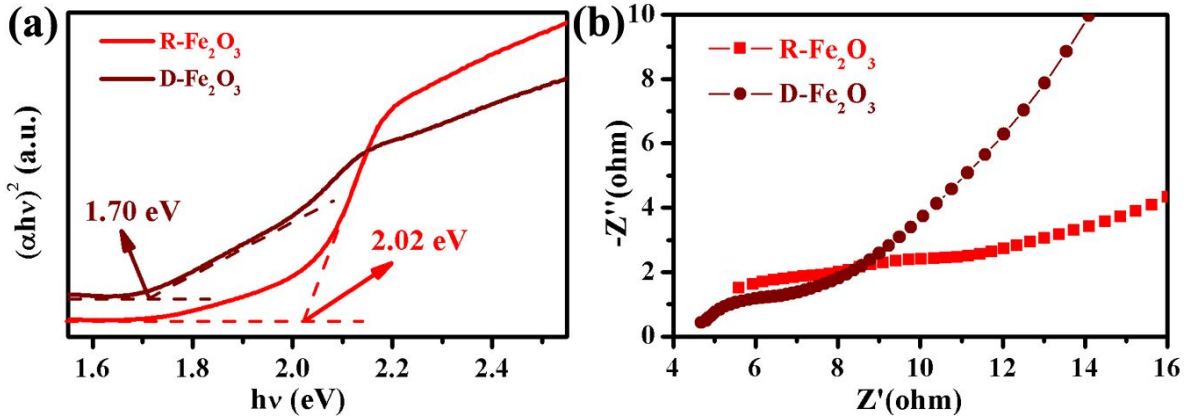

Figure S3. (a) Tauc plots evaluating the optical band gap is shown for R-Fe_2O_3 and D-Fe_2O_3 nanostructured arrays. (b) the enlargement of EIS spectra of R-Fe_2O_3 and D-Fe_2O_3 photoanodes in high frequency region.

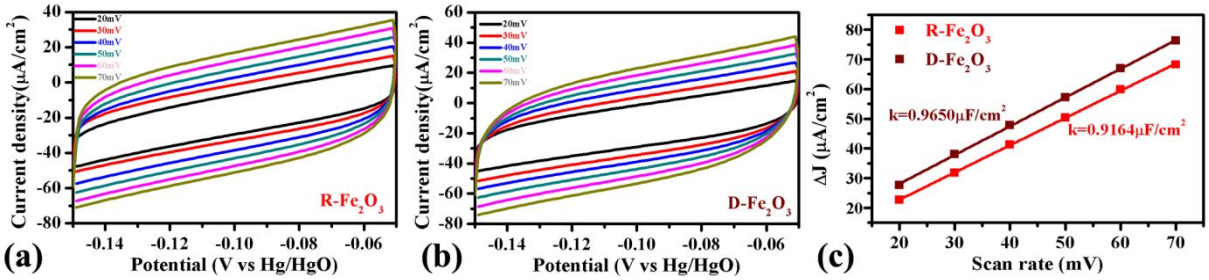

Figure S4. Linear cyclic voltammetry of R-Fe_2O_3 (a) and D-Fe_2O_3 (b) and (c) difference in current density variation plotted against scan rate.

Table S1. Comparison of PEC performance and morphology of different hematite

Material	Electrolyte	Photocurrent density(mA/cm^2)	IPCE at 366 nm	Annealing temperature	Reference
Fe_2O_3-TiO_2-40 Micro-dumbbells	1 M NaOH	0.83 (1.6 V versus RHE)	15%	500℃	[1]
$NiFe_2O_4$/Fe_2O_3 nanorods	1 M KOH	0.304 (0.6 V versus Ag/AgCl)	0.03%	500℃	[2]
Fe_2O_3 nanorods	1 M KOH	0.027 (1.23 V versus RHE)	6%	550℃	[3]
ferrihydrite modified Ti-Fe_2O_3nanorods	1 M KOH	0.71 (1.23 V versus RHE)	12%	550℃	[4]
Fe_2O_3 nanoparticles	1M NaOH	$5x10^{-4}$ (0 V versus Ag/AgCl)	0.5%	650℃	[5]
Zr-doped α-Fe2O3 nanoflakes	1 M KOH	0.52 (1.5 V versus RHE)	16%	700℃	[6]
Fe_2O_3 nanorods	1 M KOH	0.39 (1.23 V versus RHE)	9%	700℃	[7]
Fe_2O_3 nanorods	1 M NaOH	0.71 (1.23 V versus RHE)	9%	750℃	[8]
irregular Fe_2O_3 nanorods	1 M KOH	0.15 (1.23 V versus RHE)	17%	550℃	This work

Reference

(1) Zhang, P.; Yu, L.; Wen, X.;David, Lou. Construction of Heterostructured Fe_2O_3-TiO_2 Microdumbbells for Photoelectrochemical Water Oxidation. *Angew Chem.* 2018, 57, 15076-15080.

(2) Zhang, Y.; He, J.; Yang, Q.; Zhu, H.; Wang, Q.; Xue, Q.; Yu, L. Solution quenched in-situ growth of hierarchical flower-like $NiFe_2O_4$/Fe_2O_3 heterojunction for wide-range light absorption. *J Power sources.* 2019, 440, 227120.

(3) Li, C.; Huang, C. ; Chuah, X. ; Raja, D. ; Hsieh, C.; Lu, S. Ti-MOF derived $Ti_xFe_{1-x}O_y$ Shells Boost Fe_2O_3 Nanorod Cores for Enhanced Photoelectrochemical Water Oxidation. *Chem . Eng. J.* 2019, 361, 660-670.

(4) Bu, Q.; Li, S.; Wu, Q.; Bi, L.; Wang, D.; Zou, X.; Xie, T. Ferrihydrite modified Ti-Fe_2O_3 as an effective photoanode: The Role of Interface Interactions in Enhancing the Photocatalytic Activity of Water Oxidation. *ChemSusChem.*2018, 11, 3486-3494.

(5) Feriel, B.; Lotfi, D.; B. Marí.; Brahim, B. Electrodeposited chromium-doped α-Fe_2O_3 thin film for solar water splitting. Results in Physics. 2020, 102996.

(6) Rani, B.; Kumar, M.; Ravi, G.; Ravichandran, S.; Guduru, R.; Yuvakkumar, R. Electrochemical and photoelectrochemical water oxidation of solvothermally synthesized Zr-doped α-Fe_2O_3 nanostructures. *Appl. Surf. Sci.* 2019, 471, 733-744.

(7) Li, W.; Wang, K.; Yang, X.; Zhan, F.; Wang, Y.; Liu, M.; Qiu, X.; Li, J.; Zhan, J.; Li, Q.; Liu, Y. Surfactant-assisted controlled synthesis of a metal-organic framework on Fe_2O_3 nanorod for boosted photoelectrochemical water oxidation. *Chem. Eng . J.* 2020, 379, 122256.
(8) Zhang, Q.; Wang, H.; Dong, Y.; Yan, J.; Ke, X.; Wu, Q.; Xue, S. In situ growth of ultrathin Co-MOF nanosheets on α-Fe_2O_3 hematite nanorods for efficient photoelectrochemical water oxidation. Sol Energy. 2018, 171, 388-396.